Genome-wide Analysis of Differential Transcriptional and Epigenetic Variability Across Human Immune Cell Types

Simone Ecker,[1,2,*] Lu Chen,[3,4] Vera Pancaldi,[1] Frederik O. Bagger,[4,5,6] José María Fernández,[1] Enrique Carrillo de Santa Pau,[1] David Juan,[1] Alice L. Mann,[3] Stephen Watt,[3] Francesco Paolo Casale,[6] Nikos Sidiropoulos,[7,8,9] Nicolas Rapin,[7,8,9] Angelika Merkel,[10] BLUEPRINT Consortium, Henk Stunnenberg,[11] Oliver Stegle,[6] Mattia Frontini,[4,5,12] Kate Downes,[4,5] Tomi Pastinen,[13] Taco W. Kuijpers,[14,15] Daniel Rico,[1,17] Alfonso Valencia,[1,17] Stephan Beck,[2,17] Nicole Soranzo[3,4,17,*] and Dirk S. Paul[2,16,17,*]

[1]Structural Biology and Biocomputing Programme, Spanish National Cancer Research Center (CNIO), Melchor Fernández Almagro 3, 28029 Madrid, Spain
[2]UCL Cancer Institute, University College London, 72 Huntley Street, London, WC1E 6BT, UK
[3]Department of Human Genetics, Wellcome Trust Sanger Institute, Wellcome Trust Genome Campus, Hinxton, Cambridge, CB10 1HH, UK
[4]Department of Haematology, University of Cambridge, Cambridge Biomedical Campus, Long Road, Cambridge, CB2 0PT, UK
[5]National Health Service (NHS) Blood and Transplant, Cambridge Biomedical Campus, Long Road, Cambridge, CB2 0PT, UK
[6]European Molecular Biology Laboratory, European Bioinformatics Institute, Wellcome Trust Genome Campus, Hinxton, Cambridge, CB10 1SD, UK
[7]The Finsen Laboratory, Rigshospitalet, Faculty of Health Sciences, University of Copenhagen, Ole Maaløes Vej 5, 2200, Copenhagen, Denmark
[8]Biotech Research and Innovation Centre (BRIC), University of Copenhagen, Ole Maaløes Vej 5, 2200, Copenhagen, Denmark
[9]The Bioinformatics Centre, Department of Biology, Faculty of Natural Sciences, University of Copenhagen, Ole Maaløes Vej 5, 2200, Copenhagen, Denmark
[10]National Center for Genomic Analysis (CNAG), Center for Genomic Regulation (CRG), Barcelona Institute of Science and Technology, Carrer Baldiri i Reixac 4, 08028 Barcelona, Spain
[11]Department of Molecular Biology, Radboud University, Faculty of Science, Nijmegen, 6525 GA, The Netherlands
[12]British Heart Foundation Centre of Excellence, University of Cambridge, Cambridge Biomedical Campus, Long Road, Cambridge, CB2 0PT, UK
[13]Department of Human Genetics, McGill University, 740 Dr. Penfield, Montreal, H3A 0G1, Canada
[14]Blood Cell Research, Sanquin Research and Landsteiner Laboratory, Plesmanlaan 125, Amsterdam, 1066CX, The Netherlands
[15]Emma Children's Hospital, Academic Medical Center (AMC), University of Amsterdam, Location H7-230, Meibergdreef 9, Amsterdam, 1105AX, The Netherlands
[16]Cardiovascular Epidemiology Unit, Department of Public Health and Primary Care, University of Cambridge, Strangeways Research Laboratory, Wort's Causeway, Cambridge, CB1 8RN, UK
[17]Co-senior authors

*Correspondence:
S. Ecker, s.ecker@ucl.ac.uk
N. Soranzo, ns6@sanger.ac.uk
D.S. Paul, dsp35@medschl.cam.ac.uk

Abstract

Background: A healthy immune system requires immune cells that adapt rapidly to environmental challenges. This phenotypic plasticity can be mediated by transcriptional and epigenetic variability.

Results: We applied a novel analytical approach to measure and compare transcriptional and epigenetic variability genome-wide across $CD14^{+}CD16^{-}$ monocytes, $CD66b^{+}CD16^{+}$ neutrophils, and $CD4^{+}CD45RA^{+}$ naïve T cells, from the same 125 healthy individuals. We discovered substantially increased variability in neutrophils compared to monocytes and T cells. In neutrophils, genes with hypervariable expression were found to be implicated in key immune pathways and to associate with cellular properties and environmental exposure. We also observed increased sex-specific gene expression differences in neutrophils. Neutrophil-specific DNA methylation hypervariable sites were enriched at dynamic chromatin regions and active enhancers.

Conclusions: Our data highlight the importance of transcriptional and epigenetic variability for the neutrophils' key role as the first responders to inflammatory stimuli. We provide a resource to enable further functional studies into the plasticity of immune cells, which can be accessed from: http://blueprint-dev.bioinfo.cnio.es/WP10/hypervariability.

Keywords

Differential variability, phenotypic plasticity, heterogeneity, immune cells, monocytes, neutrophils, T cells, gene expression, DNA methylation

Background

Phenotypic plasticity is fundamental to human immunity, allowing rapid cellular adaptation in response to changing environmental conditions [1]. Plasticity of immune cells can be influenced by the variability of cellular traits including gene expression and DNA methylation. The stochastic nature inherent to cellular processes such as gene regulation gives rise to cell-to-cell variation, enhancing survival under adverse conditions and stress [2–4]. Environmental stimuli including temperature, hormone levels, and invading pathogens further affect the expression of genes in a tissue- and temporal-dependent fashion [2,4,5].

Rapid and effective response to a stimulus is facilitated and intensified if the cellular trait already exhibits large stochastic fluctuations in the absence of the stimulus [3]. For example, while genes involved in stress response tend to be highly variable [3,6,7], genes involved in essential cellular functions, such as protein synthesis and metabolism, demonstrate less variable expression levels [8,9].

B and T cells utilize genetic recombination to generate a highly diverse repertoire of immunoglobulins and T cell surface receptors, respectively. In addition, immune responses are driven by the variability of key signaling molecules and transcription factors not controlled by genetic factors [10,11]. Epigenetic states, including DNA methylation, also contribute to plastic gene expression during cell fate commitment, thus enhancing fitness in response to external cues [12,13].

Transcriptional and epigenetic heterogeneity that is measured across individuals emerges from different origins. While intra-individual variability can relate to different cellular properties in response to external signals, such as cell activation and communication [3,7,14], inter-individual variability can relate to differences between the individuals, including genetic makeup, age, sex,

and lifestyle. Importantly, it has also been demonstrated that inter-individual variability can serve as an appropriate proxy for intra-individual variability at the level of single cells [7,14,15].

Both transcriptional and epigenetic variability have been shown to strongly correlate with the development and progression of human diseases [12,16,17]. For example, gene expression variability has been linked to human immunodeficiency virus (HIV) susceptibility [18], neurological disorders [18,19], and cancer [20,21]. Hypervariable DNA methylation loci can be used as biomarkers to predict the risk of neoplastic transformation in stages prior to neoplasia [22,23].

The extent and functional interpretation of transcriptional and epigenetic variability has not been systematically investigated genome-wide across multiple immune cell types in the general population. Here, we applied a novel analytical approach to measure differential variability of gene expression and DNA methylation in three major immune cell types: $CD14^{+}CD16^{-}$ classical monocytes, $CD66b^{+}CD16^{+}$ neutrophils, and $CD4^{+}CD45RA^{+}$ 'phenotypically naïve' T cells. This matched panel of cell types was derived from the same 125 healthy individuals. We show that neutrophils exhibit substantially increased variability of both gene expression and DNA methylation patterns, compared to monocytes and T cells, consistent with these cells' key role as the first line of host defense. We annotated hypervariable genes and CpGs to known homeostatic and pathogenic immune processes, and further found subsets of genes correlating with genetic makeup, donor demographic and lifestyle factors. Our data further reveal potential molecular mechanisms of immune responses to environmental stimuli, and provide a resource to enable future functional studies into the phenotypic plasticity of human immune cells in health and disease.

Results

Deep molecular profiling of immune cells in the BLUEPRINT Human Variation Panel

The analyses described in this study are based on the publicly available resource provided by the BLUEPRINT Human Variation Panel [24]. The resource contains genome-wide molecular profiles of $CD14^{+}CD16^{-}$ classical monocytes, $CD66b^{+}CD16^{+}$ neutrophils, and $CD4^{+}CD45RA^{+}$ naïve T cells. These leukocyte types were chosen due to their important role in mediating immune cell processes, their relative abundance in peripheral blood allowing for examination of multiple cellular traits, as well as the availability of experimental protocols to prepare cell populations of high purity (>95%). Monocytes and neutrophils are myeloid cells that share the same bone-marrow residing granulocyte-macrophage precursor cell. Monocytes migrate to sites of infection and differentiate into macrophages and dendritic cells to induce an immune response. As part of the innate immune system, neutrophils move within minutes to sites of infection during the acute phase of inflammation. Naïve T cells are lymphoid cells that are part of the adaptive immune system, representing mature helper T cells that have not yet recognized their cognate antigen.

Across an initial cohort of 202 healthy individuals representative of the UK population, purified preparations of these primary cells were probed for gene expression using total RNA sequencing (RNA-seq) and DNA methylation using Illumina Infinium HumanMethylation450 BeadChips ('450K arrays'). Detailed information about the experimental and analytical strategies for quantifying these cellular traits are provided in the Methods section. Figures S1 and S2 give an overview of the data quality assessment of the gene expression and DNA methylation data sets, respectively. All individuals were further profiled for DNA sequence variation using whole-genome sequencing to allow for cell type-dependent, quantitative assessment of the genetic and epigenetic determinants of transcriptional variance [24].

In this study, we exploited this resource, selecting all 125 donors for whom matched gene expression and DNA methylation data sets were available across the three immune cell types. The key analytical advance of the work presented here concerns the measurement and interpretation of differential variability. That is, the identification of loci at which gene expression and DNA methylation levels show significantly greater variation within one cell type as compared to the other cell types. An overview of the study design and analytical concept is provided in Figure 1A.

Genome-wide patterns of differential gene expression variability across immune cell types

We first assessed inter-individual expression variability of 11,980 protein-coding, autosomal genes that showed robust expression in monocytes, neutrophils, and T cells (Methods). We applied an improved analytical approach for the assessment of differential variability (Methods), taking into account the strong negative correlation between mean gene expression levels and expression variability (Figure S3).

Figure 1B gives an overview of the number of identified hypervariable genes (HVGs) that are cell type-specific, shared between two, or common to all three of the studied immune cell types. Neutrophils were found to have the largest number of HVGs overall (n=1,862), as well as of cell type-specific HVGs (n=1,163). In contrast, we found only a small number of cell type-specific HVGs in monocytes and T cells (n=14 and n=3, respectively). In addition, we identified 271 genes that were highly variable across all three immune cell types using a rank-based approach (Methods). Mature neutrophils (as profiled here) show low proliferative capacity and reduced transcriptional and translational activity [25,26]. The latter could potentially impede comparable assessment of differential variability, if the relationship between variability and mean expression levels was not taken into account. Thus, using our analytical approach, we assessed and confirmed that overall reduced gene expression levels did not technically confound the observed increased variability of gene expression levels in neutrophils (Figure S3).

We then aimed to replicate the detected hypervariable gene levels in an independent sample cohort. We retrieved a gene expression data set generated using Illumina Human HT-12 v4 Expression BeadChips consisting of $CD16^+$ neutrophils derived from 101 healthy individuals [27]. Of the 11,023 gene probes assessed on the array platform, 6,138 could be assigned to a corresponding gene identifier in our data set. Neutrophil-specific hypervariable genes measured using RNA-seq were also found to be hypervariable using expression arrays in the independent cohort of healthy individuals (Figures 1C and 1D).

In summary, we devised and assessed a novel method for the identification of differential gene expression variability. Overall, we found strongly increased variability of gene expression in neutrophils compared to monocytes and T cells, and replicated the detected neutrophil-specific hypervariable gene patterns in an external cohort.

Biological significance of differentially variable genes across immune cell types

Next, we explored the characteristics of the identified hypervariable genes. We performed ontology enrichment analysis of gene sets using the GOseq algorithm [28]. This method takes into account the effect of selection bias in RNA-seq data that can arise due to gene length differences [28]. Table S1 and Table S2 summarize the annotation data of all identified HVGs and observed gene ontology enrichment patterns, respectively.

Genes showing expression hypervariability across all three cell types were enriched in biological processes related to chemotaxis, migration, and exocytosis (Table S2). For neutrophil-specific HVGs, we found gene ontology enrichment in oxidoreductase activity and cellular processes related to virus response and parasitism (Table S2). Notable genes among those with hypervariable expression values were *CD9* (Figure 2A), *CAPN2* (Figure 2B), and *FYN* (Figure 2C). *CD9* showed increased variability across all three cell types. The gene encodes the CD9 antigen, a member of the tetraspanin family. It functions as cell surface protein that forms

complexes with integrins to modulate cell adhesion and migration and mediate signal transduction [29,30]. The neutrophil-specific HVGs *CAPN2* and *FYN* encode a calcium-activated neutral protease involved in neutrophil chemotaxis [31] and a tyrosine-protein kinase implicated in intracellular signal transduction [32], respectively.

Taken together, functional enrichment of hypervariable gene sets revealed that many of the identified hypervariable genes are involved in mediating immune-related processes. This suggests that neutrophils exhibit specific gene loci that are highly adaptable to external cues.

Determinants of inter-individual cell type-specific gene expression variability

Following the discovery and characterization of genes that present hypervariable expression levels between individuals, we next aimed to delineate potential sources of heterogeneity that can be associated to differences between individuals. We hypothesized that these sources mainly relate to genetic variation, age, sex, and lifestyle factors.

First, we determined the subset of cell type-specific HVGs that correlated with genetic variants. We retrieved gene sets with a local (*cis*) genetic component designated by expression quantitative trait locus (eQTL) and variance decomposition analyses, as described in the BLUEPRINT Human Variation Panel (Figure S4A). In neutrophils, we found that 638 of the 1,163 cell-specific HVGs (55%) associate with *cis* genetic variants (Table S1), at least partly explaining the observed gene expression variability. These data are consistent with previous reports, highlighting the role of genetic variants in mediating transcriptional variance [33–35].

Second, we correlated cell type-specific HVGs with various quantitative traits measured in individual donors: demographic information (age, body mass index, and alcohol consumption); cellular parameters as assessed by a Sysmex hematology analyzer (e.g. cell count and size); and season (i.e. minimum/maximum temperature and daylight hours of the day on which blood was drawn). The results of this analysis are provided in Tables S1 and S3. In neutrophils, we identified

49 HVGs that show significant association with at least one of the measured traits (Figure 2D). For example, we found *NFX1*, a nuclear transcription factor that regulates *HLA-DRA* gene transcription [36], to associate with neutrophil granularity (Figure 2E). An increase in neutrophil granularity can be reflective of a potential infection; this parameter is routinely monitored in a clinical setting. *FYN* gene levels (reported above) were negatively correlated with neutrophil percentage (Figure 2F).

Third, we investigated whether sex was an important source of inter-individual (autosomal) gene expression variability. We found only two of the 1,163 neutrophil-specific HVGs to be differentially expressed between sexes, *SEPT4* and *TMEM63C* (Figure S5A), and high expression variability was observed for both sexes in these genes. However, in neutrophils we identified a surprisingly large number of sex-specific differentially expressed genes of small effect size, which corresponded to important immune cell functions. We present a detailed analysis of these genes below.

In conclusion, we found that genetic makeup was an important determinant of transcriptional variability. Donor demographic and lifestyle factors also contributed towards transcriptional variability.

Neutrophil-specific hypervariable genes not mediated by *cis* genetic effects

Next, we studied in detail the subset of neutrophil-specific genes that showed hypervariable expression but did not associate with local genetic variants (n=525). Although some of these genes could be mediated by distal (*trans*) genetic factors not detected in the BLUEPRINT Human Variation Panel, it is conceivable that expression heterogeneity of this gene set was primarily due to external triggers or stochastic fluctuations.

We generated a correlation matrix of expression levels of the 525 HVGs, and identified clusters of correlated genes that may act in concert or be co-regulated. The identified co-expression

network contained 259 connected genes, and consisted of three distinct gene modules (Figure 3). We inferred biological functions corresponding to the three gene modules. All modules were highly enriched for genes with important immune-related functions.

The first and largest gene module (n=105 genes, green color) showed enrichment for inclusion body, receptor signaling, and immune response activation. The second module (n=78 genes, yellow color) was enriched in biological processes related to RNA processing and chaperone binding. The third gene module (n=33 genes, red color), contained many genes with particularly high variation in their expression patterns. *RSAD2*, an interferon-inducible antiviral protein, showed highest variability, among many other interferon-inducible genes present in module three. These genes are essential in innate immune response to viral infections [37]. Gene ontology and pathway analyses of all genes in the network module further showed a strong enrichment for response to type I interferon, and several viral disease pathways including influenza A, herpes simplex, and hepatitis (Figure S6). A detailed functional annotation of all three network modules is provided in Table S4.

Sex-specific differential gene expression across immune cell types

In our analysis, we did not detect differences in mean gene expression levels between male and female donors with log-fold change ≥1 – albeit with two exceptions in neutrophils (Figure S5A). Nonetheless, when no minimum log-fold change criterion was applied, we found that sex-dependent mean expression of autosomal genes (Figure S5B) was highly abundant in neutrophils (n=3,357 genes), compared to T cells (n=895) and monocytes (n=64).

As many autoimmune diseases have a higher incidence in females, and females show generally elevated immune responses compared to males [38], we hypothesized that genes with elevated gene expression levels in females may account for the increased incidence rates. Indeed, genes with higher mean expression levels in neutrophils derived from females (n=682) were enriched in

immune response and related pathways (Table S5). In contrast, genes with increased mean expression in male donors (n=2,675) were enriched in basic cellular processes, such as RNA processing and translation (Table S5). In addition, in male donors, genes were strongly enriched in cellular compartments, such as nuclear lumen (Table S5).

Genome-wide patterns of differential DNA methylation variability across immune cell types

Following the analyses of differential gene expression variability, we then applied our improved analytical approach to determine inter-individual variability of DNA methylation levels at 440,905 CpG sites (Methods). Again, our method accounted for confounding effects due to the correlation between mean and variability measurements (Figure S7).

Concordant with our findings for gene expression variability (Figure 1B), we found that neutrophils had the largest number of hypervariable CpG positions (HVPs) overall (n=1,053), as well as cell-specific HVPs (n=261). Neutrophils and monocytes shared a considerable number of HVPs (n=380) in contrast to T cells (Figure 1E). Finally, we identified 212 HVPs common to all three cell types. An overview of the number of HVPs is shown in Figure 1E.

Following the discovery of HVPs, we examined whether these sites were overrepresented at particular gene elements and epigenomic features. To this end, we focused on cell type-specific HVPs, correlating their DNA methylation levels with distinct cellular characteristics and molecular pathways. In Table S6, we summarize the detailed annotation of all HVPs across the three profiled immune cell types. In neutrophils, we found that cell type-specific HVPs were depleted at CpG islands, which typically occur near transcription start sites ($P = 6.37\times10^{-19}$, hypergeometric test; Figure 4A), and enriched at intergenic regions ($P = 0.03$; Figure 4B).

We hypothesized that cell type-specific HVPs localize at distal gene regulatory elements such as enhancer sequences, of which many are known to be also cell type-specific [39]. To test this hypothesis, we retrieved reference chromatin state maps of primary human monocytes,

neutrophils, and T cells from the data repository provided by the BLUEPRINT Consortium [Carrillo de Santa Pau et al., BLUEPRINT Consortium, under revision]. Chromatin states are defined as spatially coherent and biologically meaningful combinations of multiple chromatin marks [40,41]. A total of five chromatin states were designated, which corresponded to functionally distinct genomic regions, namely active promoters, enhancers, and regions related to transcriptional elongation and polycomb-repression. In addition, a 'variable' chromatin state was defined here, indicating frequent changes of local chromatin structure across samples of the same cell type. Indeed, neutrophil-specific HVPs were found to be strongly enriched in the enhancer ($P = 1.32\times10^{-12}$, hypergeometric test; Figure 4C) and variable chromatin states ($P = 3.81\times10^{-8}$; Figure 4C).

Biological significance of immune cell type-specific hypervariable CpGs

To interpret the potential cellular and biological implications of cell type-specific hypervariable CpGs, we annotated the genes in close proximity to each CpG using the Genomic Regions Enrichment of Annotations Tool (GREAT) [42]. This tool is valuable in assigning putative functions to sets of non-coding genomic regions [42].

Overall, we found enrichment in gene ontology terms attributed to genes close to HVPs in a cell type-dependent context (Table S7). For example, genes located near neutrophil-specific HVPs were enriched in gene signatures related to acute *Streptococcus pneumoniae* infection and cysteine synthase activity; the latter molecular process is important to hold off infections [43]. Consistent with established neutrophil function, this suggests that the identified HVPs play a role in regulating the expression of neutrophil-specific genes in response to infection.

In Figure 4D, we provide an example of a neutrophil-specific HVP at the promoter of the *ITGB1BP1* gene, encoding the integrin beta 1 binding protein 1. Integrins are essential cell adhesion proteins that induce intracellular signaling pathways upon activation by matrix binding

[44,45]. They function as signal transducers allowing for rapid responses to cell surface signals [45]. Notably, the highlighted HVP mapped to a variable chromatin state at this locus, indicating that it influences local chromatin dynamics upon an internal or external trigger (Figure 4D).

In conclusion, we showed that cell type-specific HVPs clustered in enhancer and dynamic chromatin states at intergenic regions, suggesting they play a role in the regulation of cell type-specific gene expression programs in response to environmental changes. Genes in proximity to HVPs were enriched in gene sets relevant to important immunological functions.

Determinants of inter-individual cell type-specific DNA methylation variability

Subsequent to the identification and annotation of CpGs with hypervariable DNA methylation levels, we explored potential reasons for the discovered inter-individual DNA methylation heterogeneity.

In agreement with our findings for gene expression variability, we determined that a large proportion of cell type-specific HVPs correlated with *cis* genetic variants reported in the BLUEPRINT Human Variation Panel (Figure S4B). In neutrophils, we found that 167 of the 261 cell type-specific HVPs (64%) associated with DNA methylation quantitative trait loci (Table S6). Our data further revealed that none of the cell type-specific HVPs were differentially methylated between male and female donors. The complete numerical results of all correlation analyses are provided in Table S8.

HVPs specific to monocytes showed frequent association with seasonal effects, such as temperature and daylight (n=12/117 HVPs; Figure S8). This finding is consistent with recent analyses reporting fluctuations of gene expression levels in monocytes depending on season and circadian rhythm [46]. Many $CD4^+$ T cell-specific HVPs particularly correlated with donor age (n=14/46 HVPs; Figure S8), in line with previous findings on age-related DNA methylation changes in T cells [47,48]. These alterations are especially interesting in the context of

immunosenescence, for which dysregulation in T cell function is thought to play a crucial role [49,50]. Naïve $CD4^+$ T cells have further been reported to become progressively longer-lived with increasing age [51], which possibly also impacts their DNA methylation patterns.

Correlation of DNA methylation variability with transcriptional output

DNA methylation at active gene elements can directly control the regulation of gene expression. While methylated gene promoters usually lead to transcriptional silencing, methylated gene bodies typically lead to transcriptional activation [52]. We next aimed to probe this paradigm in the context of gene expression and DNA methylation variability.

We measured the correlation of DNA methylation variability with transcriptional output at the level of single genes. Specifically, we studied cell type-specific HVPs that map to gene promoters and bodies, correlating their DNA methylation level with the gene expression level in the same individuals. At promoters, 30.1% (range, 23.5–33.3%) of HVPs showed a negative correlation with gene expression (Figure 5A), in support of the conventional role of DNA methylation in gene repression. At gene bodies, a small subset of HVPs (5.0%; range, 0.0–10.8%) showed a positive correlation with gene expression (Figure 5B). Table S9 gives a full account of these genes and numeric results.

An example is provided in Figure 5C, showing a monocyte-specific HVP at the gene promoter of *MSR1*. At this CpG site, DNA methylation levels were significantly correlated with gene repression (BH-corrected $P < 2.2 \times 10^{-16}$, Spearman's rank correlation). *MSR1*, encoding the CD204 antigen, is involved in endocytosis of modified low-density lipoproteins.

Relationship between DNA methylation variability and gene expression variability

Finally, we examined global patterns of DNA methylation variability in relation to transcriptional variability. In neutrophils, highly variable gene expression levels were observed at promoters

exhibiting highly variable DNA methylation levels, and also at promoters showing very stable DNA methylation levels (Figure 5D). For DNA methylation variability at gene bodies, this relationship was weaker and showed a linear tendency (Figure 5E). Importantly, these global patterns were consistent across all three immune cell types (Figure S9).

To characterize these promoter regions further, we counted the number of transcription factor binding motifs at these regions (Methods). We found an accumulation of binding motifs at promoters presenting either highly variable or very stable DNA methylation levels (Figure 5F and S8). Next, we explored the properties of the 100 genes that showed both the highest expression variability and the highest DNA methylation variability at their promoters. We found that of the 100 genes in each cell type, 66 were common to all three cell types; in turn, 10 of these 66 genes encode transcription factors. For example, in neutrophils this included *ELF1*, a transcriptional regulator of genes involved in immune response signaling pathways [53]. Neutrophil-specific HVGs were also enriched at genes with promoter sequences that contain the consensus binding motif of *ELF1* (BH-corrected $P = 1.2\times10^{-5}$; MSigDB analysis).

Taken together, these results provide evidence that DNA methylation variability and gene expression variability could be mediated by the sequence-specific binding of transcription factors, such as *ELF1* in neutrophils. Future studies will be required to further investigate the functional relevance of the observed correlation.

Discussion

In this study, we investigated the transcriptional and epigenetic variability that enables immune cells to rapidly adapt to environmental changes. To this end, we devised a novel analytical strategy to assess inter-individual variability of gene expression and DNA methylation as a measure of functional plasticity across three immune cell types.

A key insight from our integrative analyses is that neutrophils exhibit substantially increased variability of both gene expression and DNA methylation compared to monocytes and T cells (Tables S1 and S6). In neutrophils, genes with important functions in intracellular signaling, cell adhesion, and motility showed increased variability (Tables S2 and S7). Importantly, a subset of these genes were found to be under epigenetic control, such as *RSAD2*, a gene involved in interferon-mediated immune response (Figure 3). Neutrophils play a diverse role in innate immune defense and act as effector cells of adaptive immunity. They use multiple sophisticated molecular mechanisms to locate and contain pathogens, including phagocytosis, degranulation, and NETosis, i.e. the generation of neutrophil extracellular traps, NETs [54,55]. The phenotypic and functional heterogeneity of neutrophils has recently been recognized [56]. Here, we add to these data, providing evidence that increased variability of gene expression and DNA methylation relate to functional diversity and effective adaptability during homeostatic and potentially pathogenic immune processes.

For our analyses we exploited the unique resource provided by the BLUEPRINT Human Variation Panel [24], enabling us to conduct the most comprehensive study of molecular variability in primary cell types to date. It allowed us to perform systematic, paired analyses across cell types and individuals, thus accounting to a large extent for potential differences related to sample processing and donor characteristics. However, we acknowledge that it is not possible to rule out a role for other confounding factors: Heterogeneity may also be partly explained by differing stages and rates of cell activation and cell death during experimental processing, as well as unaccounted environmental effects such as circadian rhythm, diet, physical activity, and psychological stress, which could affect one cell type more than the other(s).

Differences in the proportions of cellular subpopulations may contribute to overall elevated variability between individuals. We have thus assessed the expression profiles of a number of genes that identify distinct cellular subpopulations of neutrophils [56]: *CXCR4*, *CD63*, *CD62L*

(also known as *SELL*), and *CD49* (also known as *ITGA4*). We did not observe inter-individual gene expression differences of surface markers corresponding to known neutrophil subpopulations, with the exception of CD49 (Figure S10). We note that *CD49* gene expression levels did not correlate with neutrophil granularity (BH-corrected $P = 0.89$, Spearman's rank correlation). These data suggest that variation in neutrophil subpopulations is unlikely to be a main determinant of increased inter-individual variability. Future studies are required to corroborate these results and to determine whether uncharacterized cellular subpopulations may contribute to the observed heterogeneity. Novel transcriptome and epigenome profiling techniques investigating gene expression and DNA methylation variability at the level of single cells will provide valuable additional information [57–59].

We have prepared all data sets generated in this study as an easily accessible and freely available online resource, comprising all results that showed statistical significance (n=3,378) [60]. The portal is aimed to enable the research community to mine all results generated by our analyses and to conduct follow-up research into the plasticity of immune cells. In such studies, hypervariable gene-phenotype associations (Tables S3 and S8) can be further characterized using experimental approaches. For example, gene expression and DNA methylation hypervariability could be correlated to pathophysiological triggers of immune responses, such as interferon-γ and lipopolysaccharide [61].

Conclusions

We found that neutrophils show increased variability in both their gene expression and DNA methylation patterns compared to monocytes and T cells. Our data suggest that increased variability in neutrophils may lead to cellular plasticity, enabling rapid adaptation to new or changing environments such as inflammation and pathogen intrusion. A detailed molecular

421 understanding of the role of cellular heterogeneity in the human immune system is crucial to
422 specifically target a pathogenic cellular subset without compromising immunity, ultimately
423 advancing therapeutic design and treatment strategies in hematopoietic and immunological
424 diseases.

425

426 # Methods

427 ## Sample collection and cell isolation

428 As part of the BLUEPRINT Human Variation Panel, a total of 202 healthy blood donors were
429 recruited from the Cambridge NIHR BioResource [62]. Sample material was obtained at the NHS
430 Blood and Transplant Centre in Cambridge (UK) with informed consent (REC 12/EE/0040).
431 Donors were on average 55 years of age (range, 20–75 years) and 46% of donors were male. Blood
432 was processed within three hours of collection. Whole blood was used to purify $CD14^{+}CD16^{-}$
433 monocytes, $CD66b^{+}CD16^{+}$ neutrophils, and naïve $CD4^{+}CD45RA^{+}$ T cells using a multistep
434 purification strategy. The purity of each cell preparation was assessed by multi-color fluorescence-
435 activated cell sorting (FACS). Purity was on average 95% for monocytes, 98% for neutrophils,
436 and 93% for $CD4^{+}$ T cells. Purified cell aliquots were pelleted, stored at -80°C, and transported to
437 the processing institutes. Further details about the experimental protocols and quality control
438 assessments are provided by the BLUEPRINT Human Variation Panel [24].

439

440 ## RNA-sequencing assay and data preprocessing

441 RNA-seq sample preparation and library creation were performed for monocytes and neutrophils
442 at the Max Planck Institute for Molecular Genetics (Germany), and for T cells at McGill University
443 (QC, CA). Purified cell aliquots were lysed and RNA extracted using TRIZOL reagent (Life
444 Technologies) following the manufacturer's protocol. Sequencing libraries were prepared using a

TruSeq Stranded Total RNA Kit with Ribo-Zero Gold (Illumina). Adapter-ligated libraries were amplified and indexed via PCR. Libraries were sequenced using 100 bp single-end reads for monocytes and neutrophils, and paired-end reads for T cells. Reads from each RNA-seq library were assessed for duplication rate and gene coverage using FastQC [63]. Then, PCR and sequencing adapters were trimmed using Trim Galore. Trimmed reads were aligned to the GRCh37 reference genome using STAR [64]. We used GENCODE v15 to define the annotated transcriptome. Read counts of genes and exons were scaled to adjust for differences in total library size using DESeq2 [65]. Then, we applied ComBat [66] to correct for batch effects. An overview of the RNA-seq data quality assessment is provided in Figure S1.

Quantification of gene expression

Analyses on RNA-seq data were performed on exon-based read counts per gene. We omitted all genes not expressed in at least 50% of all samples in each of the three cell types, leaving only genes that were robustly expressed in all three cell types. In addition, we included only protein-coding genes, resulting in a final set of 11,980 genes. RNA-seq read counts were converted into expression log counts by applying the formula $\log_2(x+1)$.

Illumina Infinium HumanMethylation450 assay and data preprocessing

For monocytes and neutrophils, cell lysis and DNA extraction were performed at the University of Cambridge (UK), followed by bisulfite conversion and DNA methylation profiling at University College London (UK). T cells were processed at McGill University (QC, CA). DNA methylation levels were measured using Infinium HumanMethylation450 assays (Illumina) according to the manufacturer's protocol. All 450K array data preprocessing steps were carried out using established analytical methods incorporated in the R package minfi [67]. First, we performed background correction and dye-bias normalization using NOOB [68], followed by normalization

between Infinium probe types with SWAN [69]. Next, we filtered out probes based on the following criteria: (1) median detection $P \geq 0.01$ in one or more samples; (2) bead count of less than three in at least 5% of samples; (3) mapping to sex chromosomes; (4) ambiguous genomic locations [70]; (5) non-CG probes; and (6) containing SNPs (MAF ≥ 0.05) within 2 bp of the probed CG. Finally, we adjusted for batch effects using an empirical Bayesian framework [66], as implemented in the ComBat function of the R package SVA [71]. An assessment of the DNA methylation data quality is shown in Figure S2.

Quantification of DNA methylation

The final data set that passed quality control consisted of 440,905 CpG sites. DNA methylation values were represented as either M-values or β-values. The methylation M-value is the $\log_2$-ratio of the intensities of the methylated probe versus the unmethylated probe on the 450K array, while the β-value is the ratio of the methylated probe intensity and the overall intensity. All analyses of DNA methylation data were performed using M-values. Due to their easier interpretability (i.e. 0–100% DNA methylation), β-values were used for the visualization of DNA methylation data in most figures.

Analysis of differential variability

To assess differential variability across the three cell types, we applied a combined statistical approach based on DiffVar [72], which is embedded in the framework of limma [73,74]. DiffVar calculates the median absolute deviation from the group mean (MAD) of expression levels of a particular gene, or DNA methylation at a given CpG site, across all individuals for two conditions, e.g. two distinct cell types. Then, a moderated t-test is used to test for a significant increase or decrease in MAD-value between the two conditions. However, we found that the MAD variability measurement employed by DiffVar is correlated with mean levels (Figures S3 and S7), which

could potentially confound the assessment of variability. Therefore, we included an additional measurement of variability that corrects for the dependency of variability measurements on the mean [8], here referred to as EV (gene expression variability value) and MV (DNA methylation variability value). The corresponding algorithm models variance as a function of the mean, and then calculates the ratio of the observed variance to expected variance in order to get a variability measurement independent of the mean. Differential variability was tested in three group-wise comparisons. Statistical significance was defined as BH-corrected [75] P <0.05 and EV/MV difference ≥10% relative to the observed range of EV-/MV-values. For each cell type, both contrasts in which the cell type is involved were considered to define statistically significant differential variability. For example, for a gene to be a neutrophil-specific HVG, it must show significantly increased variability in both the comparison versus monocytes and versus T cells. For a gene to be classified as hypervariable across two cell types (shared hypervariability), it must exhibit significantly increased variability in the two corresponding cell types, but low variability in the third. Thus, no gene can appear in more than one list. The statistical tests were performed in a paired fashion, taking into account that all three cell types were derived from the same individuals. This procedure corrects for potential differences related to individuals and sample processing.

Analysis of variability common to all three cell types

To identify HVGs common to all three cell types, we applied a rank-based approach. We ordered both MAD- and EV-values of all genes in the three cell types from high to low variability, and then took the top n genes with highest variability across all three cell types, where n corresponds to the mean number of results obtained for the gene lists of differential variability. Specifically, n=271 for gene expression variability, and n=212 for DNA methylation variability.

520 **Gene set enrichment analyses**

521 For HVGs, we applied GOseq using the default parameters, and set 'use_genes_without_cat' =
522 FALSE, thus ignoring genes without an annotated category for the calculation of *P*-values [28].
523 With regards to HVPs, we analyzed the biological functions of flanking genes with GREAT [42]
524 using the standard parameters: association rule = basal + extension (constitutive 5 kb upstream,
525 1 kb downstream, up to 1 Mb extension); curated regulatory domains = included. In both analyses
526 we used the set of analyzed features as background, and the cutoff for statistical significance was
527 set at BH-corrected $P < 0.25$.

528

529 **Gene co-expression network and pathway analysis**

530 For neutrophil-specific HVGs not associated with *cis* genetic variants in the BLUEPRINT Human
531 Variation Panel, we first constructed a co-regulation network by calculating gene expression
532 correlations. The threshold of gene correlations was set at Pearson's $r > 0.6$. Unconnected genes
533 were removed. The resulting correlation network was then further analyzed using Cytoscape [76].
534 Clusters were identified by the agglomerative clustering method FAG-EC [77] of the ClusterViz
535 plugin. Enrichment analyses of resulting gene clusters were performed using clueGO [78], setting
536 the Kappa score to 0.4 and the cutoff for statistical significance at BH-corrected $P < 0.05$.All
537 networks were visualized using Gephi [79].

538

539 **Correlation analyses**

540 Associations between both gene expression and DNA methylation levels with donor-specific
541 quantitative traits, cellular parameters, as well as weather and seasonal effects were assessed by
542 calculating Spearman's rank correlation coefficients (rho) and their corresponding *P*-values.
543 Results were considered statistically significant at BH-corrected $P < 0.05$. This threshold was also
544 used for the correlation analyses between DNA methylation and gene expression data.

545 **Analyses of seasonal effects**

546 We downloaded historical raw weather data for the minimum and maximum daily temperature in
547 London Heathrow (UK) for the period of data collection from the National Climatic Data Centre
548 (USA) [80]. We applied linear interpolation to account for missing values. Additionally, we
549 downloaded daylight hours for London [81]. The obtained data were then correlated with gene
550 expression and DNA methylation values corresponding to the date of blood donation using
551 Spearman's rank correlation coefficient (see details above).

552

553 **Analyses of sex-specific differential gene expression**

554 In each cell type, mean gene expression and DNA methylation differences between male and
555 female donors were identified using limma [73,74]. A moderated t-test was performed and
556 statistical significance defined as BH-corrected P <0.05 and log-fold change ≥1. Results could be
557 driven by differences in menopause status between female donors. Therefore, we performed the
558 same analysis on only the subset of donors whom are younger than 50 years, and obtained very
559 similar results compared to the complete donor group.

560

561 **Functional annotation of hypervariable CpGs**

562 For the enrichment analyses with regards to gene elements and epigenomic features, we used the
563 annotation provided by the Illumina 450K array manifest. Enrichment was assessed by repeated
564 random sampling (n=1,000) using all probes that passed quality control (n=440,905).

565

566 **Transcription factor motifs analysis at gene promoter regions**

567 Consensus transcription factor binding motifs were retrieved from the database
568 'JASPAR_CORE_2016 _vertebrates.meme' [82]. Using FIMO [83], we scanned for transcription

569 factor binding motifs ($P < 1\times10^{-5}$) at promoter regions, defined as ±500 bp around the transcription
570 start site of genes listed in the reference gene set 'UCSC.hg19.knownGene'.

571

572 **Programming language**

573 If not indicated otherwise, analyses were performed using R v3 (R Development Core Team, 2008)
574 and Bioconductor [84].

575

576 # List of Abbreviations

577 HIV, human immunodeficiency virus; RNA-seq, RNA sequencing; HVG, hypervariable gene;
578 HVP, hypervariable CpG position; FACS, fluorescence-activated cell sorting; MAD, median
579 absolute deviation; EV, gene expression variability value; MV, DNA methylation variability
580 value.

581

582 # Declarations

583 **Ethics approval and consent to participate**

584 All sample material was obtained at the NHS Blood and Transplant Centre in Cambridge (UK)
585 with informed consent (REC 12/EE/0040).

586

587 **Consent for publication**

588 Not applicable.

589

590

591

592

Availability of data and materials

All data sets generated as part of this study are available at the European Genome-phenome Archive (EGA) [85] under the following accession numbers: EGAS00001001456 for 450K array data; EGAS00001000752 and EGAS00001000327 for RNA-seq data.

Competing interests

P. Flicek is a member of the Scientific Advisory Board for Omicia, Inc.

Funding

This work was funded by the EU-FP7 Project BLUEPRINT (HEALTH-F5-2011-282510).

Authors' Contributions

S. Ecker and D.S. Paul designed the study. S. Ecker, D.S. Paul, L. Chen, V. Pancaldi, F.O. Bagger, E. Carrillo de Santa Pau, D. Juan, N. Sidiropoulos, N. Rapin, and A. Merkel analyzed data. All other authors provided samples or analytical tools. D.S. Paul and S. Ecker wrote the manuscript. D. Rico, A. Valencia, S. Beck, N. Soranzo, and D.S. Paul supervised the study. All authors read and approved the final manuscript.

Acknowledgments

We would like to thank K. Pearce and M. Kristiansen (UCL Genomics) for processing the Illumina Infinium HumanMethylation450 BeadChips; D. Balzereit, S. Dökel, A. Kovacsovics, and M. Linser (Max Planck Institute for Molecular Genetics) for help with generating the RNA-seq data; B. Phipson (Murdoch Childrens Research Institute) and H.C. Bravo (University of Maryland) for advice on statistical analyses; C. Bock (CeMM Research Center for Molecular Medicine of the

Austrian Academy of Sciences) for useful discussions; A. Orozco (University of Costa Rica) for technical support; V. Naranbhai, B. Fairfax, and J. Knight (University of Oxford) for providing access to the neutrophil gene expression data set for replication; and L. Phipps for proofreading the manuscript. We gratefully acknowledge the participation of all NIHR Cambridge BioResource volunteers, and thank the Cambridge BioResource staff for their help with volunteer recruitment. We thank members of the Cambridge BioResource SAB and Management Committee for their support of our study and the NIHR Cambridge Biomedical Research Centre for funding. S. Ecker is supported by a "la Caixa" pre-doctoral fellowship. V. Pancaldi is supported by a FEBS Long-Term Fellowship. F.O. Bagger is supported by The Lundbeck Foundation. K. Downes is funded as a HSST trainee by NHS Health Education England. M. Frontini is supported by the BHF Cambridge Centre of Excellence (RE/13/6/30180). S. Beck acknowledges support from the Wellcome Trust (WT99148), a Royal Society Wolfson Research Merit Award (WM100023), and the EU-FP7 Project EPIGENESYS (257082). N. Soranzo's research is supported by the Wellcome Trust (WT098051 and WT091310), EU-FP7 Project EPIGENESYS (257082), and NIHR BRC.

BLUEPRINT Consortium: Cornelis A. Albers (Radboud University), Vyacheslav Amstislavskiy (Max Planck Institute for Molecular Genetics), Sofie Ashford (University of Cambridge), Lorenzo Bomba (Wellcome Trust Sanger Institute), David Bujold (McGill University), Frances Burden (University of Cambridge), Stephan Busche (McGill University), Maxime Caron (McGill University), Shu-Huang Chen (McGill University), Warren A. Cheung (McGill University), Laura Clarke (European Bioinformatics Institute), Irina Colgiu (Wellcome Trust Sanger Institute), Avik Datta (European Bioinformatics Institute), Oliver Delaneau (University of Geneva), Heather Elding (Wellcome Trust Sanger Institute), Samantha Farrow (University of Cambridge), Diego Garrido-Martín (Centre for Genomic Regulation), Bing Ge (McGill University), Roderic Guigo (Centre for Genomic Regulation), Valentina Iotchkova (European Bioinformatics Institute), Kousik Kundu (Wellcome Trust Sanger Institute), Tony

Kwan (McGill University), John J. Lambourne (University of Cambridge), Ernesto Lowy (European Bioinformatics Institute), Daniel Mead (Wellcome Trust Sanger Institute), Farzin Pourfarzad (Sanquin Research and Landsteiner Laboratory), Adriana Redensek (McGill University), Karola Rehnstrom (University of Cambridge), Augusto Rendon (University of Cambridge), David Richardson (European Bioinformatics Institute), Thomas Risch (Max Planck Institute for Molecular Genetics), Sophia Rowlston (University of Cambridge), Xiaojian Shao (McGill University), Marie-Michelle Simon (McGill University), Marc Sultan (Max Planck Institute for Molecular Genetics), Klaudia Walter (Wellcome Trust Sanger Institute), Steven P. Wilder (European Bioinformatics Institute), Ying Yan (Wellcome Trust Sanger Institute), Stylianos E. Antonarakis (University of Geneva), Guillaume Bourque (McGill University), Emmanouil T. Dermitzakis (University of Geneva), Paul Flicek (European Bioinformatics Institute), Hans Lehrach (Max Planck Institute for Molecular Genetics), Joost H. A. Martens (Radboud University), Marie-Laure Yaspo (Max Planck Institute for Molecular Genetics), Willem H. Ouwehand (University of Cambridge).

References

1. Yosef N, Regev A. Writ large: Genomic Dissection of the Effect of Cellular Environment on Immune Response. Science. 2016;354:64–8.

2. Elowitz MB, Levine AJ, Siggia ED, Swain PS. Stochastic Gene Expression in a Single Cell. Science. 2002;297:1183–6.

3. Lehner B, Kaneko K. Fluctuation and response in biology. Cell Mol Life Sci. 2011;68:1005–10.

4. Raser JM, O'Shea EK. Noise in Gene Expression: Origins, Consequences, and Control. Science. 2005;309:2010–3.

666 5. Snijder B, Pelkmans L. Origins of regulated cell-to-cell variability. Nat Rev Mol Cell Biol.
667 2011;12:119–25.

668 6. Blake WJ, Balázsi G, Kohanski MA, Isaacs FJ, Murphy KF, Kuang Y, et al. Phenotypic
669 consequences of promoter-mediated transcriptional noise. Mol Cell. 2006;24:853–65.

670 7. Dong D, Shao X, Deng N, Zhang Z. Gene expression variations are predictive for stochastic
671 noise. Nucleic Acids Res. 2011;39:403–13.

672 8. Alemu EY, Carl JW, Corrada Bravo H, Hannenhalli S. Determinants of expression variability.
673 Nucleic Acids Res. 2014;42:3503–14.

674 9. Basehoar AD, Zanton SJ, Pugh BF. Identification and distinct regulation of yeast TATA box-
675 containing genes. Cell. 2004;116:699–709.

676 10. Busslinger M, Tarakhovsky A. Epigenetic control of immunity. Cold Spring Harb Perspect
677 Biol. 2014;6:a024174.

678 11. Paszek P, Ryan S, Ashall L, Sillitoe K, Harper C V, Spiller DG, et al. Population robustness
679 arising from cellular heterogeneity. Proc Natl Acad Sci U S A. 2010;107:11644–9.

680 12. Feinberg AP, Irizarry RA. Stochastic epigenetic variation as a driving force of development,
681 evolutionary adaptation, and disease. Proc Natl Acad Sci U S A. 2010;107:1757–64.

682 13. Pujadas E, Feinberg AP. Regulated noise in the epigenetic landscape of development and
683 disease. Cell. 2012;148:1123–31.

684 14. Choi JK, Kim Y-J. Intrinsic variability of gene expression encoded in nucleosome
685 positioning sequences. Nat Genet. 2009;41:498–503.

686 15. Brock A, Chang H, Huang S. Non-genetic heterogeneity--a mutation-independent driving
687 force for the somatic evolution of tumours. Nat Rev Genet. 2009;10:336–42.

688 16. Hansen KD, Timp W, Bravo HC, Sabunciyan S, Langmead B, Mcdonald OG, et al.
689 Increased methylation variation in epigenetic domains across cancer types. Nat Genet.
690 2011;43:768–75.

691 17. Landau DA, Clement K, Ziller MJ, Boyle P, Fan J, Gu H, et al. Locally Disordered
692 Methylation Forms the Basis of Intratumor Methylome Variation in Chronic Lymphocytic
693 Leukemia. Cancer Cell. 2014;26:813–25.

694 18. Li J, Liu Y, Kim T, Min R, Zhang Z. Gene expression variability within and between human
695 populations and implications toward disease susceptibility. PLoS Comput Biol.
696 2010;6:e1000910.

697 19. Mar JC, Matigian NA, Mackay-Sim A, Mellick GD, Sue CM, Silburn PA, et al. Variance of
698 gene expression identifies altered network constraints in neurological disease. PLoS Genet.
699 2011;7:e1002207.

700 20. Bravo HC, Pihur V, McCall M, Irizarry RA, Leek JT. Gene expression anti-profiles as a
701 basis for accurate universal cancer signatures. BMC Bioinformatics. 2012;13:272.

702 21. Ecker S, Pancaldi V, Rico D, Valencia A. Higher gene expression variability in the more
703 aggressive subtype of chronic lymphocytic leukemia. Genome Med. 2015;7:8.

704 22. Teschendorff AE, Jones A, Fiegl H, Sargent A, Zhuang JJ, Kitchener HC, et al. Epigenetic
705 variability in cells of normal cytology is associated with the risk of future morphological
706 transformation. Genome Med. 2012;4:24.

707 23. Teschendorff AE, Liu X, Caren H, Pollard SM, Beck S, Widschwendter M, et al. The
708 Dynamics of DNA Methylation Covariation Patterns in Carcinogenesis. PLoS Comput Biol.
709 2014;10:e1003709.

710 24. Chen L, Ge B, Casale FP, Vasquez L, Kwan T, Garrido-Martin D, et al. Genetic drivers of

711 epigenetic and transcriptional variation in human immune cells. Cell. In press.

712 25. Geering B, Simon H-U. Peculiarities of cell death mechanisms in neutrophils. Cell Death
713 Differ. 2011;18:1457–69.

714 26. Subrahmanyam YVBK, Yamaga S, Prashar Y, Lee HH, Hoe NP, Kluger Y, et al. RNA
715 expression patterns change dramatically in human neutrophils exposed to bacteria. Blood.
716 2001;97:2457–68.

717 27. Naranbhai V, Fairfax BP, Makino S, Humburg P, Wong D, Ng E, et al. Genomic modulators
718 of gene expression in human neutrophils. Nat Commun. 2015;6:7545.

719 28. Young MD, Wakefield MJ, Smyth GK, Oshlack A. Gene ontology analysis for RNA-seq:
720 accounting for selection bias. Genome Biol. 2010;11:R14.

721 29. Berditchevski F. Complexes of tetraspanins with integrins: more than meets the eye. J Cell
722 Sci. 2001;114:4143–51.

723 30. Hemler ME. Tetraspanin functions and associated microdomains. Nat Rev Mol Cell Biol.
724 2005;6:801–11.

725 31. Nuzzi P, Senetar M, Huttenlocher A. Asymmetric localization of calpain 2 during neutrophil
726 chemotaxis. Mol Biol Cell. 2007;18:795–805.

727 32. Saito YD, Jensen AR, Salgia R, Posadas EM. Fyn: A novel molecular target in cancer.
728 Cancer. 2010;116:1629–37.

729 33. GTEx Consortium. The Genotype-Tissue Expression (GTEx) pilot analysis: Multitissue gene
730 regulation in humans. Science. 2015;348:648–60.

731 34. Gutierrez-Arcelus M, Ongen H, Lappalainen T, Montgomery SB, Buil A, Yurvsky A, et al.
732 Tissue-Specific Effects of Genetic and Epigenetic Variation on Gene Regulation and Splicing.

733 PLoS Genet. 2015;11:e1004958.

734 35. Kilpinen H, Waszak SM, Gschwind AR, Raghav SK, Witwicki RM, Orioli A, et al.
735 Coordinated effects of sequence variation on DNA binding, chromatin structure, and
736 transcription. Science. 2013;342:744–7.

737 36. Song Z, Krishna S, Thanos D, Strominger J, Ono S. A novel cysteine-rich sequence-specific
738 DNA-binding protein interacts with the conserved X-box motif of the human major
739 histocompatibility complex class II genes via a repeated Cys-His domain and functions as a
740 transcriptional repressor. J Exp Med. 1994;180:1763–74.

741 37. Schneider WM, Dittmann Chevillotte M, Rice CM. Interferon-Stimulated Genes: A Complex
742 Web of Host Defenses. Annu Rev Immunol. 2014;32:513–45.

743 38. Fairweather D, Frisancho-Kiss S, Rose NR. Sex differences in autoimmune disease from a
744 pathological perspective. Am J Pathol. 2008;173:600–9.

745 39. Roadmap Epigenomics Consortium. Integrative analysis of 111 reference human
746 epigenomes. Nature. 2015;518:317–30.

747 40. Ernst J, Kellis M. Discovery and characterization of chromatin states for systematic
748 annotation of the human genome. Nat Biotechnol. 2010;28:817–25.

749 41. Ernst J, Kellis M. ChromHMM: automating chromatin-state discovery and characterization.
750 Nat Methods. 2012;9:215–6.

751 42. McLean CY, Bristor D, Hiller M, Clarke SL, Schaar BT, Lowe CB, et al. GREAT improves
752 functional interpretation of cis-regulatory regions. Nat Biotechnol. 2010;28:495–501.

753 43. Dröge W, Holm E. Role of cysteine and glutathione in HIV infection and other diseases
754 associated with muscle wasting and immunological dysfunction. FASEB J. 1997;11:1077–89.

755 44. Harburger DS, Calderwood DA. Integrin signalling at a glance. J Cell Sci. 2009;122:159–63.

756 45. Miranti CK, Brugge JS. Sensing the environment: a historical perspective on integrin signal
757 transduction. Nat Cell Biol. 2002;4:E83-90.

758 46. Dopico XC, Evangelou M, Ferreira RC, Guo H, Pekalski ML, Smyth DJ, et al. Widespread
759 seasonal gene expression reveals annual differences in human immunity and physiology. Nat
760 Commun. 2015;6:7000.

761 47. Golbus J, Palellan TD, A BCR, Arbor A. Quantitative changes in T cell. Eur J Immunol.
762 1990;20:1869–72.

763 48. Heyn H, Vidal E, Ferreira HJ, Vizoso M, Sayols S, Gomez A, et al. Epigenomic analysis
764 detects aberrant super-enhancer DNA methylation in human cancer. Genome Biol. 2016;17:11.

765 49. Maue AC, Yager EJ, Swain SL, Woodland DL, Blackman MA, Haynes L. T-cell
766 immunosenescence: lessons learned from mouse models of aging. Trends Immunol.
767 2009;30:301–5.

768 50. Weng N. Aging of the Immune System: How Much Can the Adaptive Immune System
769 Adapt? Immunity. 2006;24:495–9.

770 51. Tsukamoto H, Clise-Dwyer K, Huston GE, Duso DK, Buck AL, Johnson LL, et al. Age-
771 associated increase in lifespan of naive CD4 T cells contributes to T-cell homeostasis but
772 facilitates development of functional defects. Proc Natl Acad Sci U S A. 2009;106:18333–8.

773 52. Jones PA. Functions of DNA methylation: islands, start sites, gene bodies and beyond. Nat
774 Rev Genet. 2012;13:484–92.

775 53. Gallant S, Gilkeson G. ETS transcription factors and regulation of immunity. Arch Immunol
776 Ther Exp. 2006;54:149–63.

777 54. Amulic B, Cazalet C, Hayes GL, Metzler KD, Zychlinsky A. Neutrophil Function: From
778 Mechanisms to Disease. Annu Rev Immunol. 2012;30:459–89.

779 55. Kolaczkowska E, Kubes P. Neutrophil recruitment and function in health and inflammation.
780 Nat Rev Immunol. 2013;13:159–75.

781 56. Silvestre-Roig C, Hidalgo A, Soehnlein O. Neutrophil heterogeneity: implications for
782 homeostasis and pathogenesis. Blood. 2016;127:2173–81.

783 57. Angermueller C, Clark SJ, Lee HJ, Macaulay IC, Teng MJ, Hu TX, et al. Parallel single-cell
784 sequencing links transcriptional and epigenetic heterogeneity. Nat Methods. 2016;13:229–32.

785 58. Buettner F, Natarajan KN, Casale FP, Proserpio V, Scialdone A, Theis FJ, et al.
786 Computational analysis of cell-to-cell heterogeneity in single-cell RNA-sequencing data reveals
787 hidden subpopulations of cells. Nat Biotechnol. 2015;33:155–60.

788 59. Farlik M, Sheffield NC, Nuzzo A, Datlinger P, Schönegger A, Klughammer J, et al. Single-
789 Cell DNA Methylome Sequencing and Bioinformatic Inference of Epigenomic Cell-State
790 Dynamics. Cell Rep. 2015;10:1386–97.

791 60. BLUEPRINT WP10 data portal: Hypervariability. 2016. http://blueprint-
792 dev.bioinfo.cnio.es/WP10/hypervariability. Accessed 7 Oct 2016.

793 61. Fairfax BP, Humburg P, Makino S, Naranbhai V, Wong D, Lau E, et al. Innate Immune
794 Activity Conditions the Effect of Regulatory Variants upon Monocyte Gene Expression. Science.
795 2014;343:1246949.

796 62. The Cambridge NIHR BioResource. 2016. http://www.cambridgebioresource.org.uk.
797 Accessed 7 Oct 2016.

798 63. Andrews S. FastQC A Quality Control tool for High Throughput Sequence Data. 2014.
799 http://www.bioinformatics.babraham.ac.uk/projects/fastqc/. Accessed 26 Jun 2015.

800 64. Dobin A, Davis CA, Schlesinger F, Drenkow J, Zaleski C, Jha S, et al. STAR: Ultrafast
801 universal RNA-seq aligner. Bioinformatics. 2013;29:15–21.

802 65. Love MI, Huber W, Anders S. Moderated estimation of fold change and dispersion for RNA-
803 Seq data with DESeq2. Genome Biol. 2014;15:550.

804 66. Johnson WE, Li C, Rabinovic A. Adjusting batch effects in microarray expression data using
805 empirical Bayes methods. Biostatistics. 2007;8:118–27.

806 67. Aryee MJ, Jaffe AE, Corrada-Bravo H, Ladd-Acosta C, Feinberg AP, Hansen KD, et al.
807 Minfi: a flexible and comprehensive Bioconductor package for the analysis of Infinium DNA
808 methylation microarrays. Bioinformatics. 2014;30:1363–9.

809 68. Triche TJ, Weisenberger DJ, Van Den Berg D, Laird PW, Siegmund KD. Low-level
810 processing of Illumina Infinium DNA Methylation BeadArrays. Nucleic Acids Res.
811 2013;41:e90.

812 69. Makismovic J, Gordon L, Oshlack A. SWAN: Subset-quantile Within Array Normalization
813 for Illumina Infinium HumanMethylation450 BeadChips. Genome Biol. 2012;13:R44.

814 70. Nordlund J, Bäcklin CL, Wahlberg P, Busche S, Berglund EC, Eloranta M-L, et al. Genome-
815 wide signatures of differential DNA methylation in pediatric acute lymphoblastic leukemia.
816 Genome Biol. 2013;14:r105.

817 71. Leek JT, Johnson WE, Parker HS, Jaffe AE, Storey JD. The SVA package for removing
818 batch effects and other unwanted variation in high-throughput experiments. Bioinformatics.
819 2012;28:882–3.

820 72. Phipson B, Oshlack A. DiffVar: a new method for detecting differential variability with
821 application to methylation in cancer and aging. Genome Biol. 2014;15:465.

822 73. Ritchie ME, Phipson B, Wu D, Hu Y, Law CW, Shi W, et al. limma powers differential

823 expression analyses for RNA-sequencing and microarray studies. Nucleic Acids Res.
824 2015;43:e47.

825 74. Smyth GK. Limma: Linear Models for Microarray Data. In: Gentleman R, Carey V, Dudoit
826 S, Irizarry R, Huber W, editors. Bioinformatics and computational biology solutions using R and
827 Bioconductor. New York: Springer; 2005. p. 397–420.

828 75. Benjamini Y, Hochberg Y. Controlling the False Discovery Rate: A Practical and Powerful
829 Approach to Multiple Testing. J R Stat Soc Ser B Stat Methodol. 1995;289–300.

830 76. Shannon P, Markiel A, Ozier O, Baliga NS, Wang JT, Ramage D, et al. Cytoscape: A
831 Software Environment for Integrated Models of Biomolecular Interaction Networks. Genome
832 Res. 2003;13:2498–504.

833 77. Li M, Wang J, Chen J. A fast agglomerate algorithm for mining functional modules in
834 protein interaction networks. BioMedical Engineering and Informatics. 2008. p. 3–7.

835 78. Bindea G, Mlecnik B, Hackl H, Charoentong P, Tosolini M, Kirilovsky A, et al. ClueGO: a
836 Cytoscape plug-in to decipher functionally grouped gene ontology and pathway annotation
837 networks. Bioinformatics. 2009;25:1091–3.

838 79. Bastian M, Heymann S, Jacomy M. Gephi: an open source software for exploring and
839 manipulating networks. Int AAAI Conf. 2009;

840 80. National Climatic Data Center (NCDC). 2016. http://www.ncdc.noaa.gov/cdo-web/search.
841 Accessed 8 Apr 2016.

842 81. Timeanddate.com. 2016. http://www.timeanddate.com. Accessed 8 Apr 2016.

843 82. Mathelier A, Zhao X, Zhang AW, Parcy F, Worsley-Hunt R, Arenillas DJ, et al. JASPAR
844 2014: An extensively expanded and updated open-access database of transcription factor binding
845 profiles. Nucleic Acids Res. 2014;42:D142-7.

846 83. Grant CE, Bailey TL, Noble WS. FIMO: Scanning for occurrences of a given motif.
847 Bioinformatics. 2011;27:1017–8.

848 84. Gentleman RC, Carey VJ, Bates DM, Bolstad B, Dettling M, Dudoit S, et al. Bioconductor:
849 open software development for computational biology and bioinformatics. Genome Biol.
850 2004;5:R80.

851 85. European Genome-phenome Archive. 2016. https://www.ebi.ac.uk/ega/. Accessed 7 Oct
852 2016.

853

854 **FIGURE LEGENDS**

855 **Figure 1. Differential variability of gene expression and DNA methylation across three**
856 **immune cell types**

857 (A) Study design and analytical approach. Hypervariable genes and CpGs were identified using a
858 combined statistical approach at stringent significance thresholds, i.e. Benjamini-Hochberg (BH)-
859 corrected P <0.05 and gene expression/DNA methylation variability measurement (EV/MV)
860 difference ≥10% relative to the observed range.

861 (B) Barplots showing the number of statistically significant hypervariable genes (HVGs) that are
862 cell type-specific, shared between two, or common to all three of the studied immune cell types.

863 (C) Scatter plot of the EV-values of 6,138 genes assessed in our data set versus the replication set.
864 We found good concordance between the two independent cohorts, despite the application of
865 different analytical platforms (Pearson's r = 0.48, P <2.2×10^{-16}).

866 (D) Ranking of all 11,980 protein-coding genes analyzed in our study according to EV-values (i.e.
867 from high to low EV-values). We highlight the 100 genes that showed the highest and lowest EV-
868 values in the independent replication data set in red and blue, respectively.

869 (E) Barplots showing the number of hypervariable CpG positions (HVPs).

Abbreviations: M=monocytes, N=neutrophils, T=naïve T cells.

Figure 2. Characterization of cell type-specific hypervariable genes

(A–C) Increased expression variability of the genes *CD9*, *CAPN2*, and *FYN* across three immune cell types. For each cell type, data points represent the expression values of the indicated gene in one individual. Cell types marked by an arrow were found to show significantly increased variability compared to the other two cell types. While *CD9* was found to be hypervariable in all three cell types, *CAPN2* and *FYN* show increased variability only in neutrophils, if contrasted to monocytes and T cells.

(D) Heatmap of Spearman's correlation coefficients showing neutrophil-specific HVGs that associated with various donor-specific quantitative traits. A total of 49 genes with increased inter-individual variability showed a significant association with at least one of the measured traits (BH-corrected P <0.05, Spearman's rank correlation).

(E) Scatter plot of *NFX1* gene expression levels versus neutrophil granularity.

(F) Scatter plot of *FYN* gene expression levels versus neutrophil percentage.

Figure 3. Gene network and pathway analysis of neutrophil-specific HVGs not mediated by *cis* genetic effects

Co-expression network of neutrophil-specific HVGs that did not correlate with genetic variants in *cis*, as reported in the BLUEPRINT Human Variation Panel. We identified three gene modules, shown in green, yellow, and red. These modules were highly enriched for important biological functions in immune cells (Table S4). Nodes represent genes, and edges represent correlations in these genes' expression values. Node sizes are determined by expression variability of the corresponding gene, with bigger nodes indicating higher EV-values. Nodes colored in gray belong to several smaller gene clusters connecting the three main clusters of the network.

Figure 4. Functional annotation of neutrophil-specific hypervariable CpG positions

(A) Enrichment of neutrophil-specific HVPs (n=261) at genomic features. We found neutrophil-specific HVPs to be depleted at CpG islands ($P = 6.37\times10^{-19}$, hypergeometric test).

(B) Enrichment of neutrophil-specific HVPs at gene elements. Neutrophil-specific HVPs were enriched at intergenic regions ($P = 0.03$).

(C) Enrichment of neutrophil-specific HVPs at distinct reference chromatin states in neutrophils. The HVPs were enriched at enhancer ($P = 1.32\times10^{-12}$) and 'variable' ($P = 3.81\times10^{-8}$) chromatin states. A 'variable' chromatin state denotes a state that was observed in less than 80% of the biological replicates (n ≥5) within a given cell type, and indicates dynamic changes of local chromatin structure.

(D) Regional plot of an exemplar neutrophil-specific HVP mapping to the promoter of the *ITGB1BP1* gene, encoding the integrin beta 1 binding protein 1. The statistically significant HVP is indicated with an arrow. For each cell type, data points represent the DNA methylation β-values (y-axis) at the indicated CpGs (x-axis) in one individual. For each CpG site, we calculated the mean DNA methylation value (indicated with a larger data point). Every CpG site is annotated with regards to genomic feature, gene element, and chromatin state.

Abbreviations: M=monocytes, N=neutrophils, T=naïve T cells, TSS=transcription start site, CGI=CpG island, UTR=untranslated region, prom=promoter.

Figure 5. Relationship between DNA methylation and gene expression

(A) Barplots showing the proportion of cell type-specific HVPs that map to gene promoters and are positively (red), negatively (blue), or not (white) associated with gene expression levels at BH-corrected P <0.05 (Spearman's rank correlation). We found that around one third of these HVPs (30.1%; range 23.5–33.3%) is negatively correlated with gene expression.

(B) Barplots as shown in panel (A) but for HVPs that map to gene bodies.

(C) Scatter plot showing the negative correlation of *MSR1* promoter DNA methylation with gene expression in monocytes (r = -0.70, $P < 2.2 \times 10^{-16}$; Spearman's rank correlation).

(D) Correlation between DNA methylation variability and gene expression variability at gene promoters in neutrophils. First, gene-wise MV-values were calculated. Then, the values were ordered from low to high MV-value, grouped together in bins of 100 genes, and plotted against the EV-values, maintaining the ordering by MV-values. This binning strategy was applied to reduce the complexity of the data. HVPs at gene promoters were defined as CpG sites annotated to TSS1500, TSS200, 5'UTR, and first exon, according to the Illumina 450K array annotation manifest. Darker data points indicate the subset of bins that is further discussed in the Results section.

(E) Same scatter plot as shown in panel (D) but for HVPs that map to gene bodies. HVPs at gene bodies were defined as CpGs annotated to body and 3'UTR, according to the 450K array annotation manifest.

(F) Scatter plot of the number of consensus transcription factor binding motifs at promoter regions versus MV-values in neutrophils. Promoter regions were defined as ±500 bp around the transcription start site. Darker data points indicate the subset of bins that is further discussed in the Results section.

Abbreviations: MV=DNA methylation variability, TF=transcription factor.

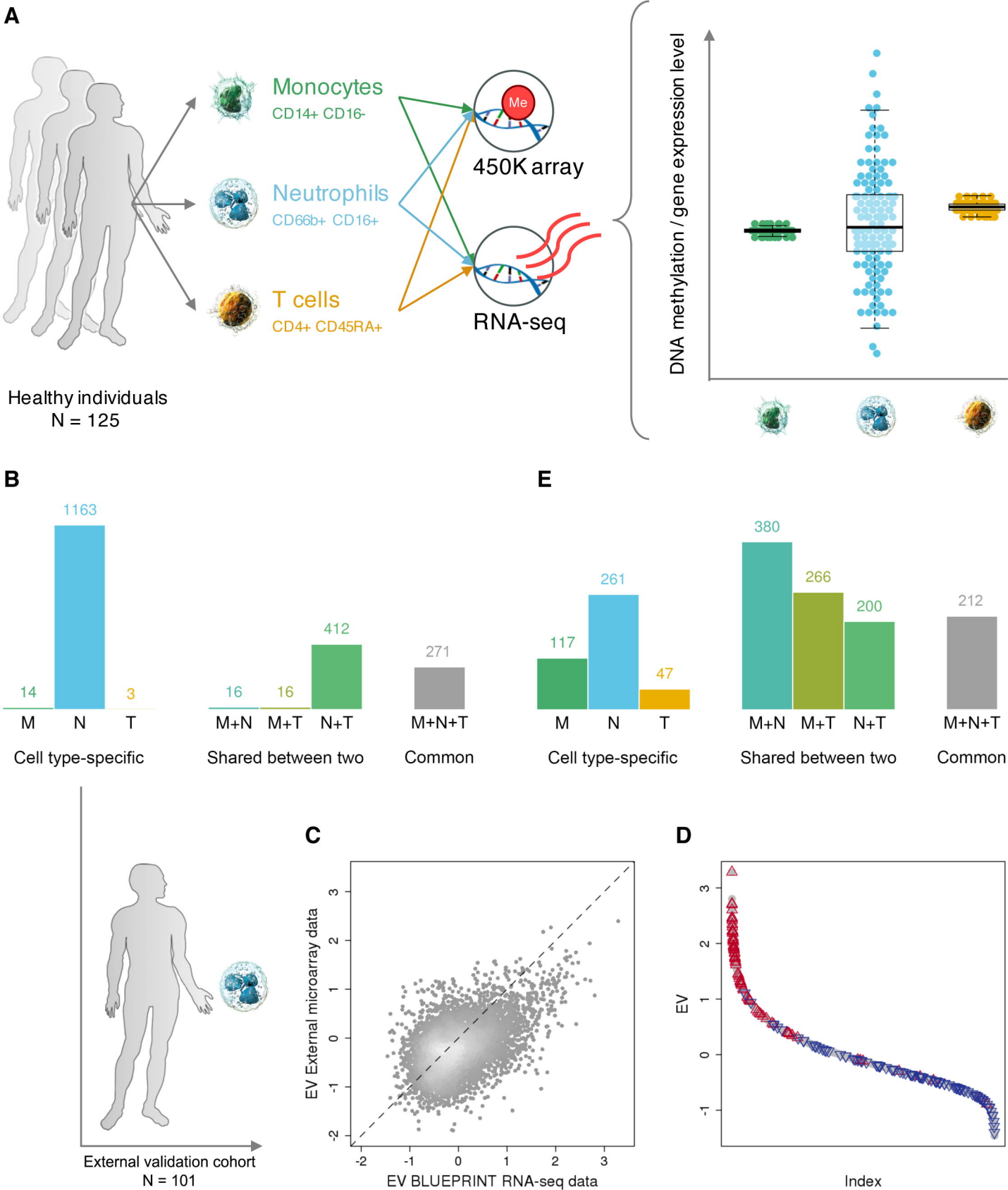
A
Monocytes
CD14+ CD16-
Neutrophils
CD66b+ CD16+
T cells
CD4+ CD45RA+
Me
450K array
RNA-seq
Healthy individuals
N = 125
DNA methylation / gene expression level
B
1163
14
3
412
16
16
271
M
N
T
M+N
M+T
N+T
M+N+T
Cell type-specific
Shared between two
Common
E
261
117
47
380
266
200
212
Cell type-specific
Shared between two
Common
External validation cohort
N = 101
C
EV External microarray data
EV BLUEPRINT RNA-seq data
D
EV
Index

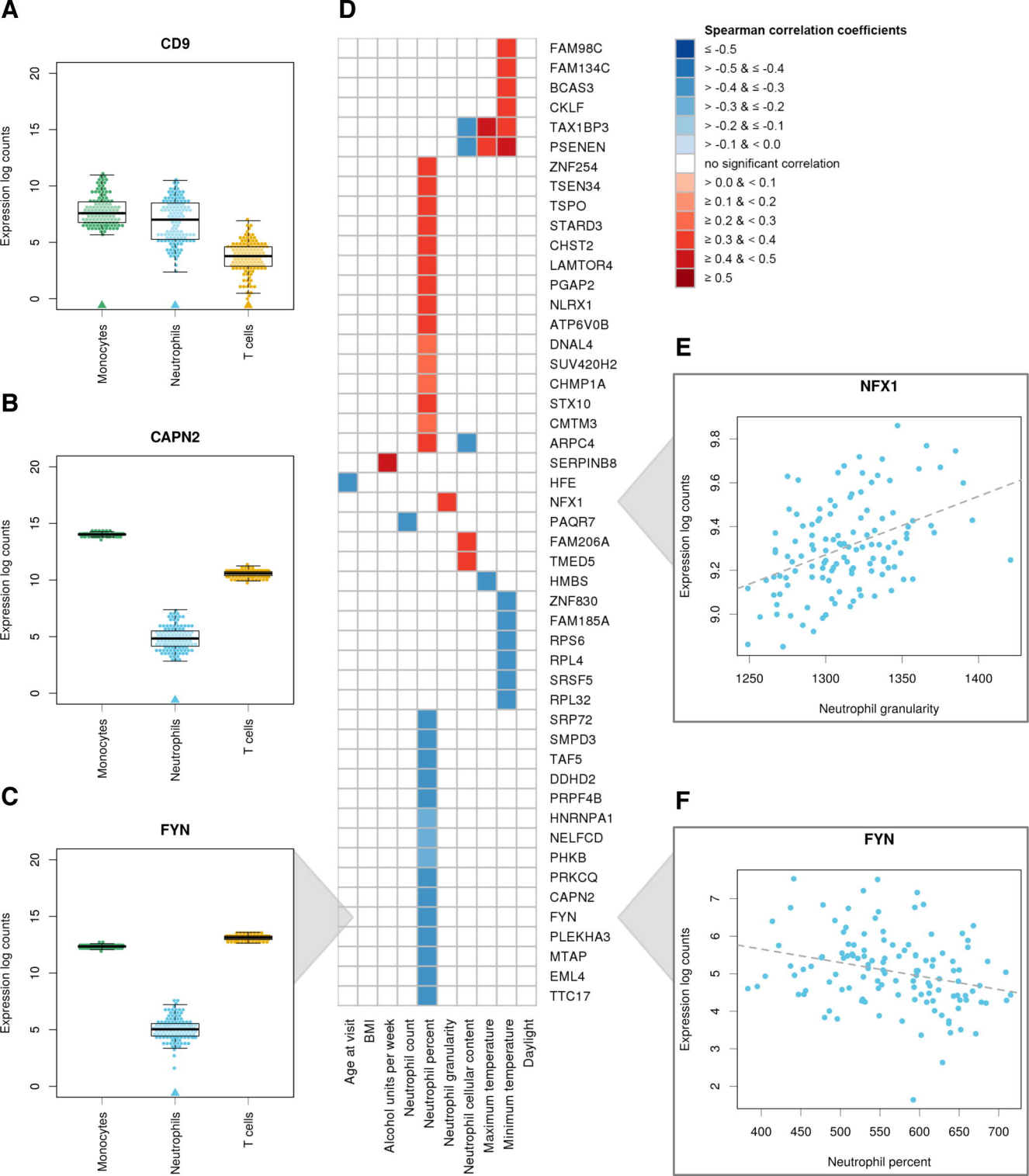
A
CD9
Expression log counts
Monocytes
Neutrophils
T cells
B
CAPN2
C
FYN
D
Spearman correlation coefficients
≤ -0.5
> -0.5 & ≤ -0.4
> -0.4 & ≤ -0.3
> -0.3 & ≤ -0.2
> -0.2 & ≤ -0.1
> -0.1 & < 0.0
no significant correlation
> 0.0 & < 0.1
≥ 0.1 & < 0.2
≥ 0.2 & < 0.3
≥ 0.3 & < 0.4
≥ 0.4 & < 0.5
≥ 0.5
FAM98C
FAM134C
BCAS3
CKLF
TAX1BP3
PSENEN
ZNF254
TSEN34
TSPO
STARD3
CHST2
LAMTOR4
PGAP2
NLRX1
ATP6V0B
DNAL4
SUV420H2
CHMP1A
STX10
CMTM3
ARPC4
SERPINB8
HFE
NFX1
PAQR7
FAM206A
TMED5
HMBS
ZNF830
FAM185A
RPS6
RPL4
SRSF5
RPL32
SRP72
SMPD3
TAF5
DDHD2
PRPF4B
HNRNPA1
NELFCD
PHKB
PRKCQ
CAPN2
FYN
PLEKHA3
MTAP
EML4
TTC17
Age at visit
BMI
Alcohol units per week
Neutrophil count
Neutrophil percent
Neutrophil granularity
Neutrophil cellular content
Maximum temperature
Minimum temperature
Daylight
E
NFX1
Expression log counts
Neutrophil granularity
F
FYN
Expression log counts
Neutrophil percent

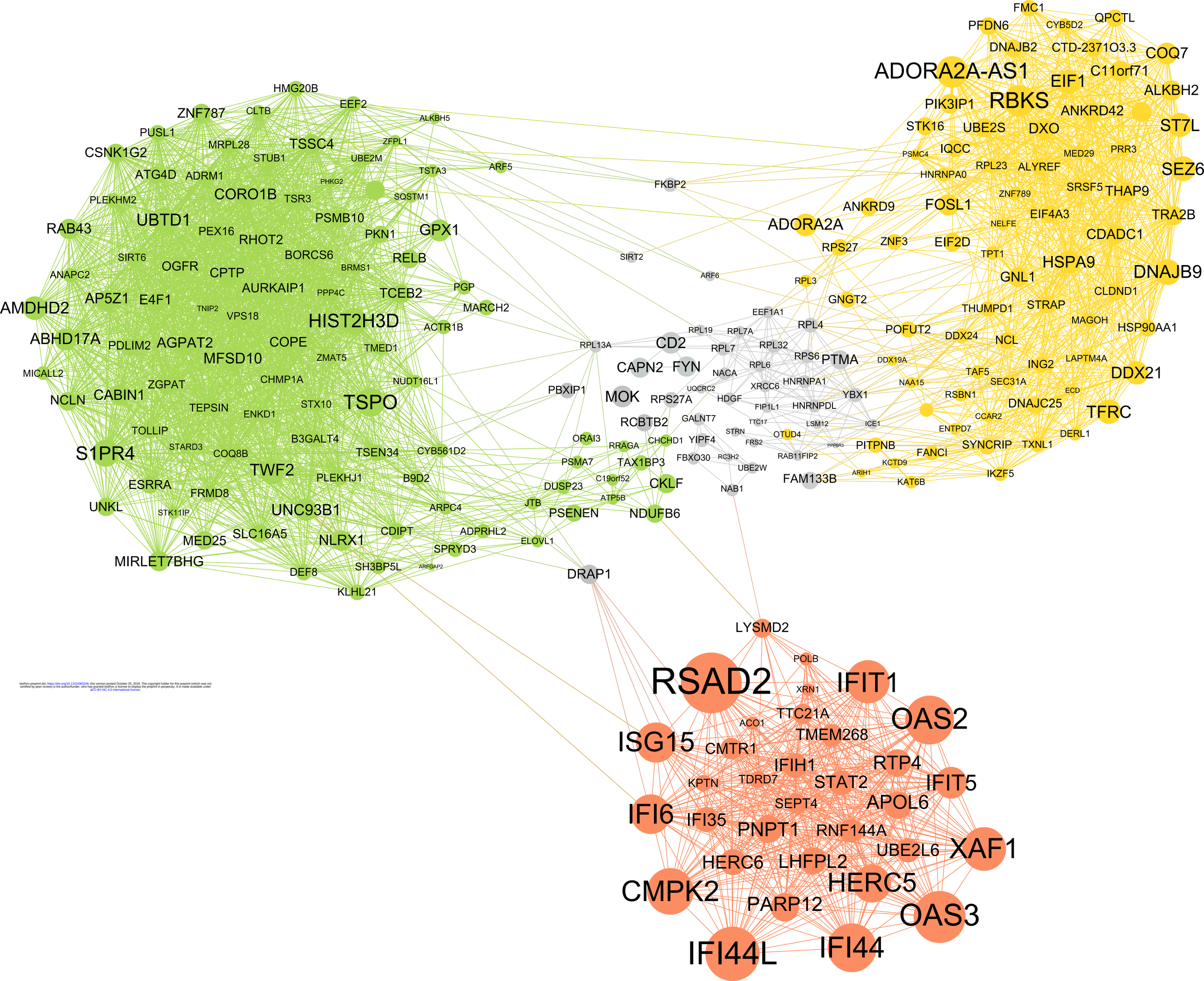

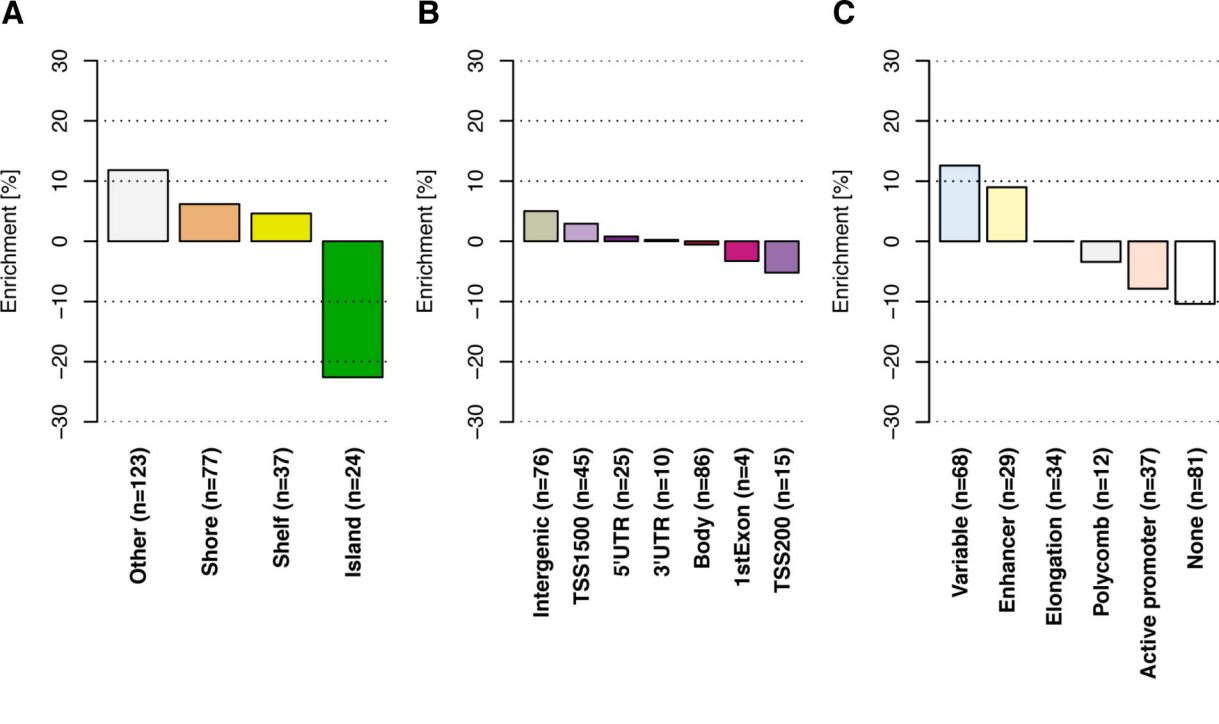
A
B
C
Enrichment [%]
30
20
10
0
−10
−20
−30
Other (n=123)
Shore (n=77)
Shelf (n=37)
Island (n=24)
Intergenic (n=76)
TSS1500 (n=45)
5'UTR (n=25)
3'UTR (n=10)
Body (n=86)
1stExon (n=4)
TSS200 (n=15)
Variable (n=68)
Enhancer (n=29)
Elongation (n=34)
Polycomb (n=12)
Active promoter (n=37)
None (n=81)

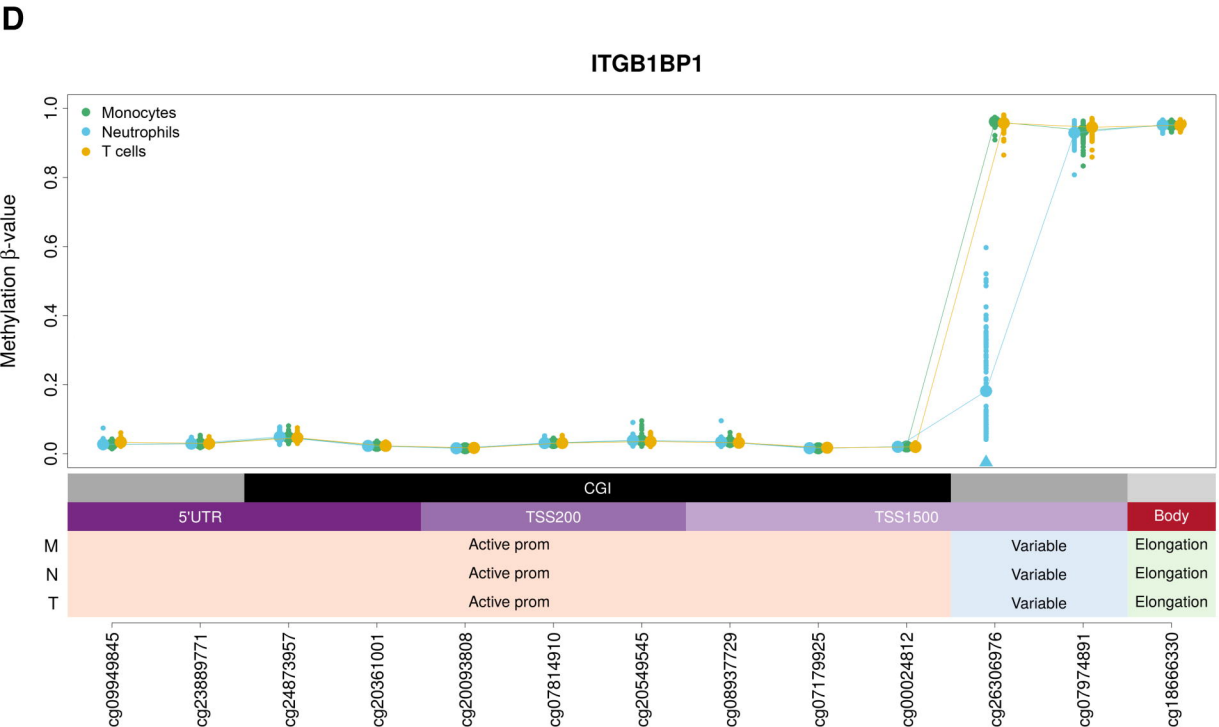
D
ITGB1BP1
Monocytes
Neutrophils
T cells
Methylation β-value
1.0
0.8
0.6
0.4
0.2
0.0
CGI
5'UTR
TSS200
TSS1500
Body
M
N
T
Active prom
Variable
Elongation
cg09949845
cg23889771
cg24873957
cg20361001
cg20093808
cg07814910
cg20549545
cg08937729
cg07179925
cg00024812
cg26306976
cg07974891
cg18666330

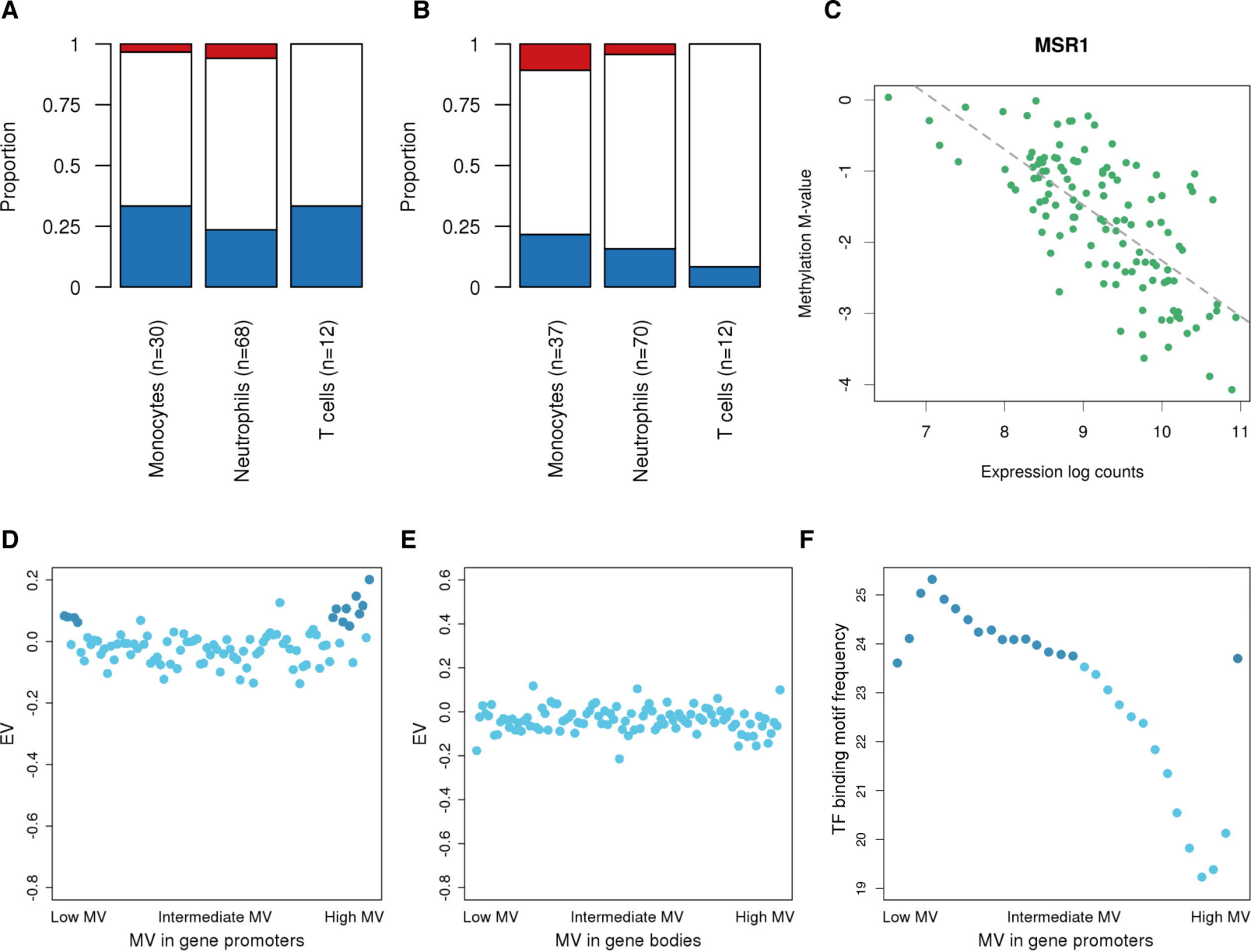
A
B
C
Proportion
1
0.75
0.5
0.25
0
Monocytes (n=30)
Neutrophils (n=68)
T cells (n=12)
Monocytes (n=37)
Neutrophils (n=70)
T cells (n=12)
MSR1
Methylation M-value
0
-1
-2
-3
-4
7
8
9
10
11
Expression log counts
D
E
F
EV
0.2
0.0
-0.2
-0.4
-0.6
-0.8
0.6
0.4
Low MV
Intermediate MV
High MV
MV in gene promoters
MV in gene bodies
TF binding motif frequency
25
24
23
22
21
20
19